Canadian Mineralogist
Vol. 14, pp. 32-39 (1976)

EXPERIMENTAL MODELLING OF INTER-ELEMENTAL RELATIONSHIP IN NATURAL FERROMANGANESE MATERIALS

V. SUBRAMANIAN
School of Theoretical and Environmental Sciences, Jawaharlal Nehru University, New Delhi - 110057, India.

ABSTRACT

An experimental investigation was made on the multiple hydroxide coprecipitation of Fe, Mn and Ni from aqueous media of varying ionic strength. The coprecipitates were studied with the aid of several analytical tools, including infrared spectra, Mössbauer effects and the scanning electron microscope.

The results indicate that the coprecipitates represent structural mixing among the end members. Thermodynamic calculations suggest the presence of a continuous solid solution in a binary system involving any two of the three components Fe $(OH)_3$, $Mn(OH)_2$ and $Ni(OH)_2$ as the end members. Free energies of mixing calculated from the experimental data indicate that the mixed hydroxides are stable relative to the pure end members.

The mixed hydroxides have certain exchange capacity which is dependent on the ionic strength of the aqueous media. Trace elements such as Co and Cu in the aqueous media can occupy these exchange sites.

The solid-solution model and exchange reactions developed on the basis of the experimental results could be used to satisfactorily explain the positive inter-elemental relationship between Fe and Mn and also the negative relationship between (Fe+Mn) and the trace elements in natural ferromanganese materials.

RÉSUMÉ

Une enquête expérimentale a été faite sur la coprécipitation multiple d'hydroxide de Fe, Mn et Ni d'un milieu aqueux de résistance ionique variante. Les co-précipités ont été étudiés à l'aide de différents instruments analytiques, tels les spectres infrarouges, les effets de Mössbauer et le microscope électronique à balayage.

Les résultats indiquent que les co-précipités représentent un mélange structural parmi les membres extrêmes. Des calculs thermodynamiques suggèrent la présence d'une solution solide continue dans un système binaire incluant deux des trois composants $Fe(OH)_3$, $Mn(OH)_2$ et $Ni(OH)_2$ comme extrêmes. Les énergies libres, du mélange calculé des données de l'expérience, indiquent que les hydroxydes mélangés sont stables par rapport aux hydroxydes extrêmes purs.

Les hydroxydes mélangés ont une certaine capacité d'échange qui dépend de la résistance ionique du milieu aqueux. Des éléments de trace, tels Co et Cu dans le milieu aqueux, peuvent occuper ces sites d'échange.

Le modèle de solution solide et les réactions d'échange développés sur la base des résultats expérimentaux pourraient être utilisés pour expliquer de façon satisfaisante le rapport inter-éléments positif entre Fe et Mn ainsi que le rapport négatif entre (Fe+Mn) et les éléments de trace dans des matériaux de ferromanganèse naturels.

(Traduit par le journal)

INTRODUCTION

The ability of hydroxide coatings to act as sinks for various trace metals is well-known (Gibbs 1973; Jenne 1967; Kharkar *et al.* 1968; Martin *et al.* 1973). Inter-elemental relationships among the several elements in coatings and other ferromanganese materials have been reported (Cronan & Thomas 1972) but a proper explanation of such correlation, *i.e.*, negative or positive correlation between any two elements, is lacking.

Hem (1972), Kharkar *et al.* (1968), Morgan & Stumm (1965) and several others proposed that ferric hydroxide precipitate absorbs other cations such as Mn^{2+}, Ni^{2+} and Co^{2+} from a solution and eventually fixes them by solid-state diffusion. The possibility of solid solution between two or more components in ferromanganese materials has been suggested (Burns 1965; Crerar & Barnes 1974; Loganathan & Burau 1973) but has not been investigated in detail.

In coatings and other ferromanganese materials, significant quantities of Fe and Mn occur as hydroxides (Gibbs 1973). In order to understand the inter-elemental relationship in such hydroxides, laboratory experiments were performed which involved the coprecipitation of hydroxides of Fe, Mn and Ni and the study of the properties of the aqueous media and also of the precipitates. Attempts have been made in this paper to relate the experimental observations to the chemistry of natural ferromanganese materials.

Experimental Procedures

The laboratory work is schematically illustrated in Figure 1. Details of individual experiments outlined in the flow chart are presented elsewhere (Subramanian 1973). All experiments were done at room temperature and pressure. All containers for the aqueous media and for the precipitates were kept sealed to prevent oxidation. Elemental analyses were done with a Laboratory Instruments Model Atomic Absorption Spectrophotometer. Measurement of pH was done with a Beckman pH meter using glass-calomel electrodes. All washings were done with double-distilled deionized water. All solutions for elemental analyses were kept refrigerated after acidifying to pH less than 3. Various analytical tools were employed in studying the precipitates and are described in individual sections.

Results and Discussion

Precipitation of mixed hydroxides

In order to investigate the nature of hydroxide coprecipitation from solutions of varying ionic strength, Fe-Mn-Ni hydroxides were coprecipitated, following the procedure outlined in Figure 1, from solutions of ionic strength approximating that of world-average river water (Livingstone 1963), sea water, and mixtures of the two in various proportions.

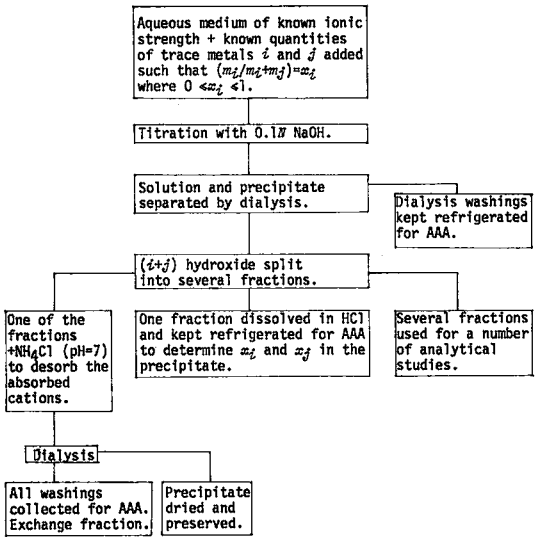

FIG. 1. A generalized flow chart for the experimental work. Aqueous media used include synthetic river water, synthetic sea water, various mixtures of the two, and double-distilled deionized water. *i* and *j* represent any two of the three elements considered: Fe, Mn and Ni; *m* and *x* are the concentration in solution and mole fraction in the solid respectively, AAA is atomic-absorption analysis.

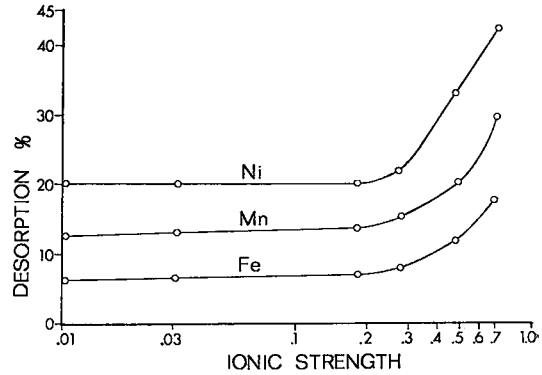

FIG. 2. Desorption of Fe, Mn and Ni from a coprecipitated Fe-Mn-Ni hydroxide. Desorption is expressed as % weight loss from the precipitate.

Desorbable cations from a precipitate are a measure of its exchange capacity. In addition, a small amount of the precipitate will dissolve in the medium in which desorption takes place. Thus, the precipitate loses its exchange fraction, and also the small soluble fraction, to the aqueous media. Figure 2 shows the variations in the total cations released from the mixed precipitates formed from solutions of varying ionic strength. Only from precipitate formed from aqueous media comparable to that of sea water does the desorption appear significant for Fe. On the other hand, a constant but significant amount of Mn and Ni are released from precipitates formed even from dilute solutions. The precipitates can be considered to contain two fractions — the exchangeable fraction and the non-desorbable "fixed" fraction. The relative proportions of these fractions in the precipitates vary with the ionic strength of the precipitating medium. As the ionic strength of the aqueous media increases to that of sea water, the exchange fraction increases at the cost of the "fixed" fraction in the precipitate. This leads one to expect wide compositional variations in the ferromanganese materials formed from saline waters as compared to those formed from fresh waters.

Properties of the mixed hydroxide precipitates

Infrared spectra. Spectra were taken with KBr discs and a Beckman Model 5 IR Double

TABLE 1. INFRARED SPECTRA DATA

Mole Fraction of Mn in $Fe(OH)_3$	Positions of Maximum Absorption Peaks (cm^{-1})
0.0 - Pure $Fe(OH)_3$	600, 650(D)*, 850(D)
0.02	600, 650(D) , 850(D)
0.05	600, 650(D) , 850
0.08	600, 850
0.145	600, 850
0.22	600, 850
0.33	600, 850
0.44	500
0.50	500
0.55	600, 850 (D)
0.60	550, 860
0.70	500, 600, 850 (D)
0.80	500, 650, 850
1.0 - Pure Mn hydroxide	600, 650 (D), 850

*Doublet

Beam Spectrophotometer. Table 1 lists the various absorption-peak positions observed for the vibrational frequencies of the Fe-O and Mn-O bonds in the Fe-Mn hydroxide coprecipitates. The lack of significant variations in these band positions in the $Fe(OH)_3$ coprecipitated with varying amounts of Mn is in agreement with observations for natural ferromanganese materials by Elderfield & Glasby (1973). In the far infrared spectral region, where Fe-O-Fe, Mn-O-Mn, and Fe-O-Mn bands can be observed, a systematic shift in the Fe-O-Mn band was found to take place, as shown in Figure 3. The formation of a separate Mn phase, such as $Mn(OH)_3$ or MnO_2, is unlikely to account for the shift observed as Mn increases in the precipitate.

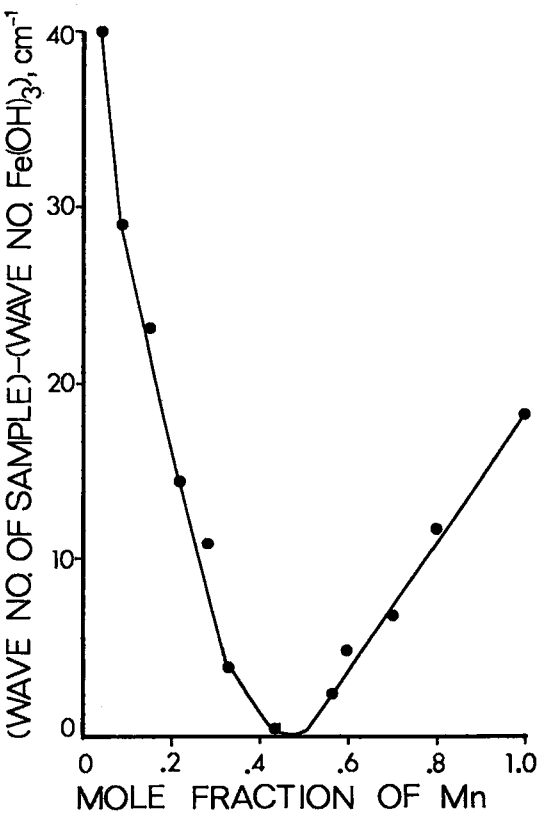

FIG. 3. Absorption-peak position of the Fe-O-Mn band for the Fe-Mn hydroxides, plotted against the mole fraction of Mn in the precipitate.

Mössbauer effects. Details of Mössbauer studies of a complete range of Fe-Mn hydroxides — from the Fe end member to the Mn end member — are reported elsewhere (Subramanian 1975a). Discussions related to the experimental model proposed in this paper are summarized as follows:

(a) Even in precipitates containing up to 80 wt % Mn, only Fe^{3+} is present; substances such as manganese ferrate or iron manganate are not precipitated by the method employed in the present study.

(b) There is more than one type of Fe^{3+} in the precipitates; ferric ions are distributed among more than one type of sites in the precipitate. It is also possible that coprecipitation gives rise to polycrystalline particles.

(c) Based on the quadrupole splitting changes with the Mn content of the precipitates, it is concluded that the grain size of the precipitate decreases from the Fe end member towards the Mn end members; Mn-rich $Fe(OH)_3$ precipitates are finer than the pure $Fe(OH)_3$. Phase changes could also accompany this size change but could not be studied due to the *x*-ray amorphous nature of the Fe-Mn hydroxides.

X-ray diffraction patterns. All the Fe-Mn hydroxide mixed precipitates — from the Fe end member to the Mn end member — were amorphous to *x*-rays. Hem (1963) similarly found some Fe-Mn coprecipitates to be amorphous to *x*-rays, but he also detected hydrohausmanite in some samples. Since Fe-Ni and Mn-Ni hydroxides are not very important in nature, they were not studied in detail by the various analytical methods employed in this work.

Scanning electron microscope studies. In the *x*-ray mapping technique utilizing the SEM, it is well known that the depth of penetration of the *x*-ray beam is a function of the beam current; elemental distribution, as recorded by the mapping technique, depends on the depth of penetration of the beam. The element distribution is also related to the surface morphology of the grain (Subramanian 1975b). By varying the electron-beam current, it is possible to count the elemental concentration up to a desired depth of penetration (Conference on Scanning Electron Microscope, 1968).

In the present work, Mn was counted with Kα radiation at various beam currents for a Fe-Mn precipitate containing equal mole percentages of Fe and Mn. Figure 4 shows the variations in Mn counts at different beam currents. The plot suggests that Mn distribution at various depths of the precipitate is uniform. The linear relationship indicates that Mn is not enriched in selective occluded areas within the precipitate. Thus, Mn in the Fe-Mn precipitate cannot be accounted for by the possible occupancy of defective sites by Mn.

Inter-elemental relationship in natural ferromanganese materials. In most natural ferromanganese materials, Fe and Mn are negatively correlated to each other (Cronan & Thomas 1972). Data for a number of environments — such as fresh water, estuarine, lacustrine and oceanic — indicate that Fe and Mn are mutually exclusive in these materials. Structurally mixed coprecipitation of Fe and Mn compounds or the absorption of Mn and $Fe(OH)_3$ and its eventual incorporation in the structure of $Fe(OH)_3$ could conveniently account for the negative correlation between Fe and Mn. The small but variable exchange capacity of the mixed precipitate, as was shown in Figure 1, could explain the presence of elements such as Co, Cu, Zn *etc.*, in the ferromanganese materials, since the total amount of trace elements in these materials is positively correlated to the total amount of (Fe+Mn).

A solid-solution model. Based on the analytical evidence and arguments presented so far, a solid solution model has been developed

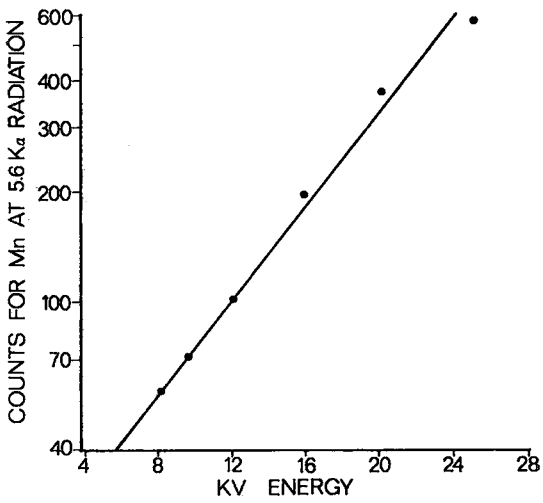

FIG. 4. Mn counts for a Fe-Mn precipitate plotted against the incident electron-beam current. Mn counted for 400 seconds using K_α radiation.

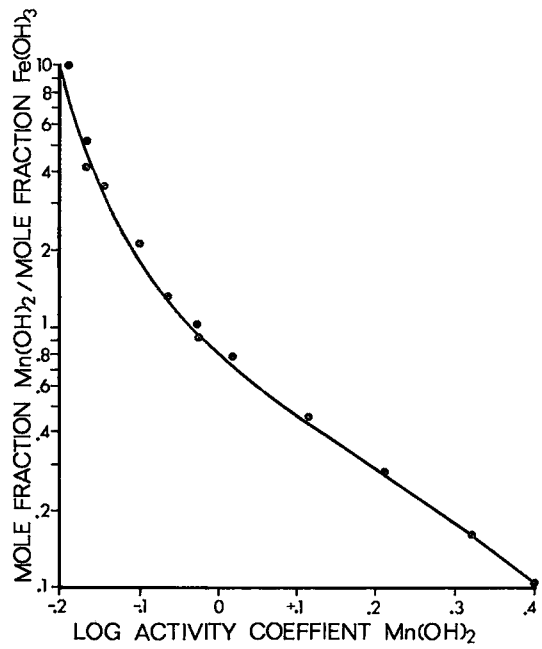

FIG. 5. Plot of the Gibbs-Duhem equation for the activity coefficient of the Mn component in the Fe-Mn precipitate. The activity coefficient for the Fe component is obtained by graphically integrating the area bounded by the curve and the two axes.

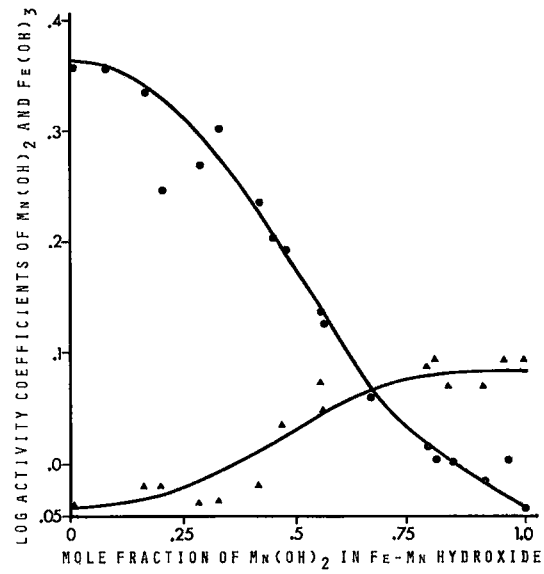

FIG. 6. The activity coefficients values for the Mn and Fe components in Fe-Mn hydroxide plotted against their mole fractions. Dots are for Mn and triangles for Fe.

TABLE 2. A SOLID-SOLUTION MODEL

If i represents a trace or minor component such as Mn and j represents the major component such as Fe, then the selectivity coefficient of i between an aqueous phase and a solid phase such as $Fe(OH)_3$ can be represented by:

$$S_j^i = (\bar{X}_i/\bar{X}_j)\cdot(C_j/C_i) \quad \text{.....(1)}$$

and the partition coefficient D is given by:

$$D_j^i = (\bar{X}_i/\bar{X}_j)\cdot(C_j/C_i)\cdot(K_i/K_j)\ (\bar{Y}_i/\bar{Y}_j) \quad \text{.....(2)}$$

where K_i and K_j are equilibrium solubility products of $Mn(OH)_2$ and $Fe(OH)_3$ respectively; $\bar{Y}$ represents the corresponding activity coefficients in the solid phases; $\bar{X}$ and C represent the equilibrium mole fraction and concentration, respectively, in the solid and aqueous phases. Equation (2) assumes that the activity coefficients of dissolved species, of interest in the present study, in the dilute solutions equal unity.

Also, given $\bar{X}_i+\bar{X}_j = 1$,

and the Gibbs-Duhem equation

$$\ln \bar{Y}_j = -\int_{\bar{X}_i=1}^{\bar{X}_i} (\bar{X}_i/\bar{X}_j)\, d \ln \bar{Y}_i \quad \text{.....(3)}$$

the activity coefficients of the two components in the hydroxide precipitate can be calculated as described below:

K_i and K_j values can be obtained from standard references; though the K values depend on the grain size (Langmuir & Whitmore 1971), lack of size information for the Fe-Mn hydroxide precipitates in the present work dictated the use of free energy of formation values from Garrels & Christ (1965) for calculating the K values. As a first approximation, let the selectivity coefficient obtained by substituting the experimental data in equation (1) be equal to the partition coefficient D_j^i. Also, assuming that the activity coefficient of the major component, $\bar{Y}_j$, equals unity, equation (2) can be solved for $\bar{Y}_i$, for corresponding values of $\bar{X}_i$. These $\bar{Y}_i$ values can be used to obtain $\bar{Y}_j$ by the graphical integration of equation (3).

Figure 5 shows the plot of equation (3) for the Fe-Mn hydroxides. The graphical integration of the area bounded by the curve and the axes yields the value of 1.59 for $\bar{Y}_j$. This value can now be used in equation (2) and a new set of $\bar{Y}_i$ values calculated. The recalculated $\bar{Y}_i$ values are now used in equation (3) as before and graphical integration gave a new value of 1.62 for $\bar{Y}_j$. Due to this small change in the $\bar{Y}_j$ value on second iteration of equations (2) and (3), no further iterations were performed. Details of iterations of the equations (2) and (3) are given in the Appendix.

The final $\bar{Y}_i$ values obtained through the above exercise can then be used, along with the following relationships, (Guggenheim 1967, p. 170-219), to obtain $\bar{Y}_j$ values for corresponding values of $\bar{X}_j$:

$$\ln \bar{Y}_i = A_0\bar{X}_i^2 + A_1(1-4\bar{X}_i^2)\bar{X}_j^2 \quad \text{.....(4)}$$

and

$$\ln \bar{Y}_j = A_0\bar{X}_j^2 - A_1(1-4\bar{X}_j^2)\bar{X}_i^2 \quad \text{.....(5)}$$

In the above equations, A_0 and A_1 are constants and their values can be derived by writing equation (4) for two values of $\bar{X}_i$ ($\bar{X}_{i(1)}$ and $\bar{X}_{i(2)}$) and $\bar{Y}_i$ ($\bar{Y}_{i(1)}$ and $\bar{Y}_{i(2)}$) and simultaneously solving for A_0 and A_1; these A values can then be used in equation (5) to obtain $\bar{Y}_j$ corresponding to two values of $\bar{X}_j$. Details of the calculations are shown in the Appendix; the A values obtained for $\bar{X}_i$ values of .165 and .2 are: $A_0 = 0.9$ and $A_1 = -.278$.

Figure 6 shows the $\bar{Y}$ values for the Mn component calculated through the iteration of equations (2) and (3) and for the Fe component calculated through the solution of equations (4) and (5). A highly non-ideal solid solution is predicted from the Figure. Free energies of mixing can be calculated through the following relationships:

$$a = \bar{X}.\bar{Y} \quad \text{.....(6)}$$

and

$$G_m = RT\sum_{i,j} \bar{X}_{i,j} \ln a_{i,j} \quad \text{.....(7)}$$

where 'a' represents the thermodynamic activity, and G_m the free energy of mixing.

(Table 2) for the mixed precipitation of any two out of the three hydroxides considered, namely, $Fe(OH)_3$, $Mn(OH)_2$ and $Ni(OH)_2$. The model is explained with the data obtained for the Fe-Mn hydroxides since these are the geologically significant systems in the sedimentary processes. For the other two binary systems, Fe-Ni and Mn-Ni hydroxides, the results shown (Figs. 9, 10) are based on similar approach.

The concentration of Mn in the Fe-Mn precipitates can be plotted against the activity of the Mn component and also against the free energy of mixing calculated through the equations in Table 2. Such plots are shown in Figures 7 and 8. The activity-concentration plots for the Ni-bearing hydroxides are shown in Figures 9 and 10.

It is clear from these figures that a complete range of solid solution exists for each of the systems considered. Ni-bearing hydroxides show either an ideal behavior or a negative departure from ideality at higher Ni concentrations. Due to the rarity of Ni-enriched Fe or Mn hydroxides, such departures have not been investigated in the present work.

From Figure 8 it is clear that the Fe-Mn hydroxides containing a large amount of both Fe and Mn have the lowest free energies of mixing compared to the pure end members. Thus, when an aqueous phase contains these two elements in quantity, the stable solid phase is likely to be a structurally-mixed Fe+Mn hydroxide rather than two separate phases of Fe and Mn.

Some applications to natural ferromanganese materials. Metallic coatings of hydroxides on sediments constitute up to 10% by weight of the sediments. Considering the total suspended solids transported to world oceans, a quantitative evaluation of the importance of coatings can be made.

Annual discharge of rivers = 3.6×10^{16} litre/year (Garrels & Mackenzie 1970)

Total dissolved Fe: 0.05 ppm (Gibbs 1972)

Solution transport of Fe: 18×10^{11} g/year

Annual suspended load: 183×10^{14} g/year (Holeman 1968)

Coatings on sediments (upper limit): 10% by weight (Jenne 1967)

Total coating transport of Fe: 10.2×10^{12} g/year

Fe (coating)/Fe (solution) = 500. Similarly, Mn (coating)/Mn (solution) = 34, and Ni (coating)/Ni (solution) = 25.

From the data of Gibbs (1973) for coatings for the Yukon and Amazon rivers, the ratio of (coating/solution) transport can be calculated

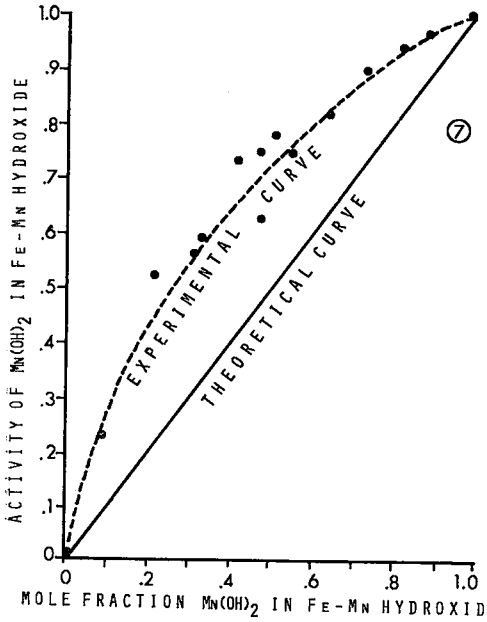

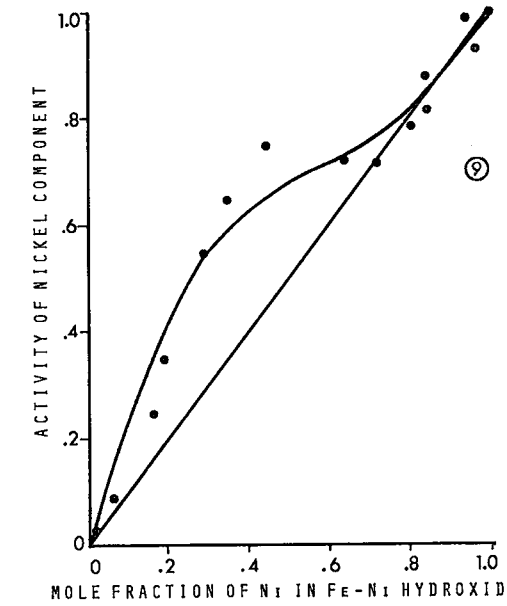

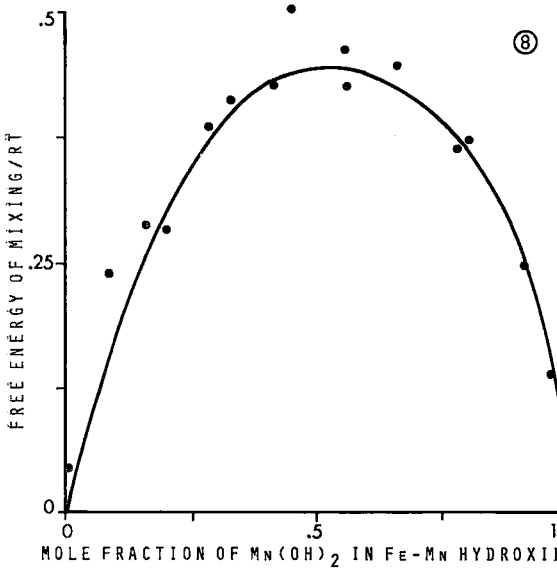

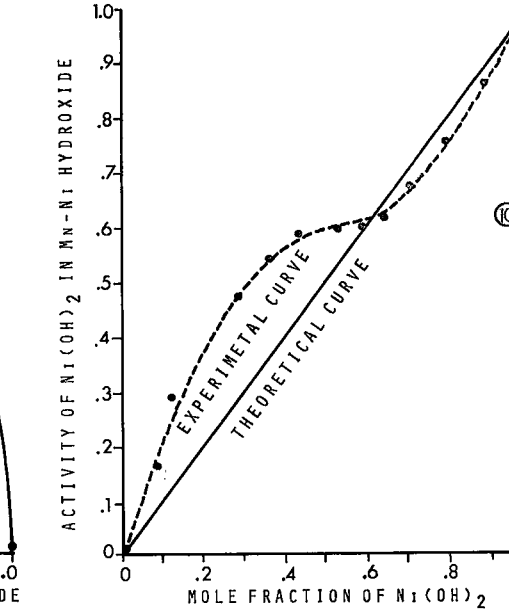

FIG. 7. Activity-composition plot for the Fe-Mn precipitates. Solid line represents theoretical ideal behaviour.

FIG. 8. Values for the free energy of mixing for the Fe-Mn hydroxides.

FIG. 9. Activity-concentration plot for the Fe-Ni hydroxides.

FIG. 10. Activity-concentration plot for the Mn-Ni hydroxides.

as 73 to 812 times for Fe, 3 to 5 times for Mn, and 22 to 24 times for Ni. The values reported earlier are in agreement with these ratios.

Fe and Mn have a mutual catalytic effect in the coprecipitation of their hydroxides (Morgan & Stumm 1965; Hem 1963). The pH control of the hydroxide precipitation is also well-known (Garrels & Christ 1965; Langmuir & Whitmore 1971; Subramanian 1973). A small change in the pH of the aqueous phase may cause some shift in the composition of the mixed precipitate through reactions such as

$$x\mathrm{Fe}^{2+} + (1-x)\,\mathrm{Mn}^{2+} + (2+x)\,(\mathrm{OH})^{1-} = [x\mathrm{Fe}\,(\mathrm{OH})_3 \cdot (1-x)\,\mathrm{Mn}\,(\mathrm{OH})_2] + xe^- \quad (8)$$

$$[x\mathrm{Fe}(\mathrm{OH})_3\,(1-x)\,\mathrm{Mn}(\mathrm{OH})_2] + y\mathrm{Mn}^{2+} + y(\mathrm{OH})^{1-} = y\mathrm{Fe}^{2-} + [x-y)\,\mathrm{Fe}(\mathrm{OH})_3 \cdot (1-x+y)\,\mathrm{Mn}\,(\mathrm{OH})_2] + ye^- \quad (9)$$

Equation (8) characterizes the formation of a Fe-Mn double hydroxide with the mole fractions of the Fe and Mn components equal to x and $(1\text{-}x)$ respectively; equation (9) characterizes the alteration of this double hydroxide, in response to pH changes, to the one in which their mole fractions are equal to $(x\text{-}y)$ and $(1\text{-}x+y)$ respectively. The above mechanism can account for the wide compositional variations in natural ferromanganese nodules.

Bonatti (1971), Cronan & Thomas (1972) and Subramanian & d'Anglejan (1975) have shown that interstitial waters of bottom sediments are enriched in transition elements. Even though the concentration of any one element may be below the solubility products of its stable solid phase under the given conditions, removal or addition of the element to the water may be through reactions outlined in equations (8) and (9).

Even though $Mn(OH)_2$ is not a stable phase (Bricker 1965), Mn could be removed by $Fe(OH)_3$ during coprecipitation, as the hydroxide component within the structurally-mixed precipitate. Elemental migration within the interstitial column (Bonatti 1971) could be in response to shifts in the equilibrium between the interstitial water and the exchange fraction of the mixed precipitate.

The presence of cations other than Fe, Mn and Ni in the coatings and other ferromanganese materials can be explained as follows: coprecipitated hydroxides contain some percentage of exchangeable fraction; the amount of this fraction varies depending on the ionic strength of the aqueous media. Cations such as Cu^{2+}, Co^{2+} and other compatible ions in the solution can replace the exchangeable Fe^{2+}, Mn^{2+} and Ni^{2+} from the absorption sites and thereby become part of the mass of the ferromanganese materials.

Conclusion

A complete range of non-ideal solid solution exists between $Fe(OH)_3$ and $Mn(OH)_2$; a limited range of solid solution is indicated for the Ni-bearing hydroxides. Due to their extremely fine size (<100Å), the Fe-Mn hydroxides are amorphous to x-ray diffraction; increase in the Mn content causes the mean size of the precipitate to decrease. pH-controlled reactions between an aqueous phase and a mixed hydroxide precipitate can cause two or more ferromanganese materials to coexist. A combination of solid solution and exchange reaction can satisfactorily explain the observed chemistry of natural ferromanganese materials.

Acknowledgement

I am grateful for the discussions I had with Ron Gibbs, Fred Mackenzie and Abraham Lerman during the course of this work.

References

Bonnatti, E. (1971): Post depositional mobility of some transition elements, P, U, Th in deep sea sediments. *Geochim. Cosmochim. Acta* **35**, 3-24.

Bricker, O. P. (1965): Some stability relations in the system $Mn\text{-}O_2\text{-}H_2O$ at 25°C and one atmosphere pressure. *Amer. Mineral.* **50**, 1296-1354.

Burns, R. G. (1965): Co in $Fe(OH)_3$. *Nature* **205**, 999.

Conference on Scanning Electron Microscope (1968): Methods and Applications. Om Johari, Director, *I.I.T. Res. Inst.*, 397 p.

Crerar, D. L. & Barnes, H. L. (1974): Deposition of deep sea Mn nodules. *Geochim. Cosmochim. Acta* **38**, 279-301.

Cronan, D. S. & Thomas, R. L. (1972): Geochemistry of ferromanganese oxide concretions and associated deposits in Lake Ontario. *Bull. Geol. Soc. Amer.* **83**, 1493-1502.

Elderfield, H. & Glasby, G. (1973): Infrared spectra of Mn nodules. *Chem. Geol.* **11**, 117-122.

Garrels, R. M. & Mackenzie, F. T. (1970): *Evolution of Sedimentary Rocks.* Norton & Co., New York. 397 p.

——— & Christ, C. L. (1965): *Solutions, Minerals and Equilibria.* Harper & Row, New York. 450 p.

Gibbs, R. J. (1973): Mechanisms of trace metals transport in rivers. *Science* **180**, 79-83.

——— (1972): Water chemistry of the Amazon river. *Geochim. Cosmochim. Acta* **36**, 785-791.

GUGGENHEIM, E. A. (1967): *Thermodynamics.* North Holland Publ., Amsterdam, 170-219.

HEM, J. D. (1972): Chemical factors that influence the availability of iron and manganese in natural waters. *Bull. Geol. Soc. Amer.* 83, 443-450.

———— (1963): Co-precipitation of Fe and Mn oxides. *Amer. Chem. Soc. Div. Water Waste Chem.*, preprint 7-10.

HOLEMAN, J. (1968): Sediment yield of world rivers. *Water Resources Research* 4, 437-447.

JENNE, E. A. (1967): Control on Mn, Fe, Co, Ni, Cu and Zn concentrations in soils and waters. *Amer. Chem. Soc. Spec. Publ.* 73, 337-387.

KHARKAR, K., TUREKIAN, K. & BERTINE, K. (1968): Stream supply of dissolved silver, molybdenum, antimony, selenium, chromium, cobalt, rubidium, and cesium to world oceans. *Geochim. Cosmochim. Acta* 32, 285-298.

LANGMUIR, D. & WHITMORE, D. (1971): Precipitation of Fe oxyhydroxides. *Amer. Chem. Soc. Spec. Paper* 106, 207-223.

LIVINGSTONE, D. A. (1963): Chemical composition of rivers and lakes. *U.S.G.S. Prof. Paper* 440G.

LOGANATHAN, P. & BURAU, R. G. (1973): Sorption of heavy metal ions by hydrous Mn oxides. *Geochim. Cosmochim. Acta* 37, 1277-1293.

MARTIN, J. M., KULBICKI, G. & DEGROOT, A. J. (1973): Terrigenous supply of radioactive and trace elements to the oceans. *Hydrogeochemistry.* Clarke & Co., New York, 443-463.

MORGAN, J. & STUMM, W. (1965): Role of multivalent oxides in limonological transformations. *Adv. Water Poll. Res.* 1, 195-230.

SUBRAMANIAN, V. (1975a): Mössbauer effects in Fe-Mn precipitates. *Physica Status Solidi (a)*, 27, p 303-308.

———— (1975b): Origin of surface pits on quartz as revealed by scanning electron microscopy. *J. Sed. Petrology* 45, 234-239.

———— & D'ANGLEJAN, B. F. (1975): Water chemistry of the St. Lawrence estuary. *J. Hydrology* (in press).

———— (1973): *Mechanisms of Fixation of the Trace Metals Mn and Ni by Ferric Hydroxide.* Ph.D. thesis, Northwestern Univ. Evanston.

Manuscript received June 1975, emended December 1975.

APPENDIX

Assuming that the activity coefficients of the dissolved ions in dilute solutions equal 1, equation (2) in the text can be re-written as:

$$D_{Fe}^{Mn} = (\bar{X}_{Mn(OH)_2}/\bar{X}_{Fe(OH)_3})/(C_{Mn}/C_{Fe}) \cdot (K_{Fe(OH)_3}/K_{Mn(OH)_2}) \cdot (\bar{Y}_{Fe(OH)_3}/\bar{Y}_{Mn(OH)_2}) \quad \ldots\ldots\ldots(2a)$$

Knowing the following data

$Y_{Mn^{2+}} = Y_{Fe^{2+}} = 0.99$; $K_{Fe(OH)_3} = 10^{38}$; $K_{Mn(OH)_2} = 10^{15.3}$ and assuming that $\bar{Y}_{Fe(OH)_3} = 1$, equation (2) can be solved with the D values obtained through the substitution of experimental values in equation (1), to get a series of values for $\bar{Y}_{Mn(OH)_2}$ for the entire range of $\bar{X}_{Mn(OH)_2}$ where $0 < \bar{X}_{Mn(OH)_2} < 1$.

These Y values for Mn can then be used in equation (3) re-written as:

$$\ln \bar{Y}_{Fe(OH)_3} = \int_{\bar{X}_{Fe(OH)_3}=1}^{\bar{X}_{Fe(OH)_3}} (\bar{X}_{Mn(OH)_2}/\bar{X}_{Fe(OH)_3})\, d \ln \bar{Y}_{Mn(OH)_2} \quad \ldots\ldots\ldots(3a)$$

and the $\bar{Y}$ values for the Fe component can be obtained by graphical integration.

The purpose of the above exercise is to obtain a value for the activity coefficient of the Fe component so that this can be substituted into equation (2a) to obtain refined values, on successive iterations, for the activity coefficient of the Mn component. Such $\bar{Y}$-Mn values can then be used along with the following equations:

$$\ln \bar{Y}_{Mn(OH)_{2(1)}} = A_0 \bar{X}^2_{Mn(OH)_{2(1)}} + A_1 (1 - 4\bar{X}^2_{Mn(OH)_{2(1)}}) \bar{X}^2_{Fe(OH)_{3(1)}} \quad \ldots(4a)$$

and

$$\ln \bar{Y}_{Mn(OH)_{2(2)}} = A_0 \bar{X}^2_{Mn(OH)_{2(2)}} + A_1 (1 - 4\bar{X}^2_{Mn(OH)_{2(2)}}) \bar{X}^2_{Fe(OH)_{3(2)}} \quad \ldots(4b)$$

to obtain the values of the constants A_0 and A_1 which can then be used to get $\bar{Y}$ values for the Fe component using the relationship

$$\ln \bar{Y}_{Fe(OH)_{3(1)}} = A_0 \bar{X}^2_{Fe(OH)_{3(1)}} - A_1 (1 - 4\bar{X}^2_{Fe(OH)_{3(1)}}) \bar{X}^2_{Mn(OH)_{2(1)}} \quad \ldots(5a)$$

and

$$\ln \bar{Y}_{Fe(OH)_{3(2)}} = A_0 \bar{X}^2_{Fe(OH)_{3(2)}} - A_1 (1 - 4\bar{X}^2_{Fe(OH)_{3(2)}}) \bar{X}^2_{Mn(OH)_{2(2)}} \quad \ldots(5b)$$

The calculations are best illustrated with the following example: from experimental data and the solution of equations (2a) and (3a),

$\bar{X}_{Mn(OH)_{2(1)}} = .165$; $\bar{Y}_{Mn(OH)_{2(1)}} = .36$; $\bar{X}_{Fe(OH)_{3(1)}} = .835$;

and

$\bar{X}_{Mn(OH)_{2(2)}} = .2$; $\bar{Y}_{Mn(OH)_{2(2)}} = .34$; $\bar{X}_{Fe(OH)_{3(2)}} = .8$;

The unknowns $\bar{Y}_{Fe(OH)_{3(1)}}$ and $\bar{Y}_{Fe(OH)_{3(2)}}$ can be calculated using these data and solving first equations (4a) and (4b) to get $A_0 = .9$ and $A_1 = -.278$. Using these A-values, in equations (5a) and (5b),

$\bar{Y}_{Fe(OH)_{3(1)}}$ = the activity coefficient of the Fe component (when the mole fraction of the Fe component = .835)
= 1.05 and

$\bar{Y}_{Fe(OH)_{3(2)}}$ = the Y value for the Fe component when its mole fraction is .8
= 1.04.

Similar calculations can be made at other concentrations of Fe.